photochem

MDPI

Communication

Demonstration of a Stereospecific Photochemical Meta Effect

Hoai Pham [1], Madelyn Hunsley [2], Chou-Hsun Yang [3], Haobin Wang [3] and Scott M. Reed [3,*]

[1] Department of Chemistry, University of Colorado Boulder, Boulder, CO 80309, USA; Hoai.Pham@colorado.edu
[2] Pfizer Boulder Research & Development, Boulder, CO 80301, USA; mlhunsley@gmail.com
[3] Department of Chemistry, University of Colorado Denver, Denver, CO 80204, USA; chou.yang@ucdenver.edu (C.-H.Y.); haobin.wang@ucdenver.edu (H.W.)
* Correspondence: scott.reed@ucdenver.edu; Tel.: +1-303-315-7634

Abstract: A fundamental goal of photochemistry is to understand how structural features of a chromophore can make specific bonds within a molecule prone to cleavage by light, or photolabile. The meta effect is an example of a regiochemical explanation for photolability, in which electron donating groups on an aromatic ring cause photolability selectively at the meta position. Here, we show, using a chromophore containing one ring with a meta-methoxy group and one ring with a para-methoxy group, that two stereoisomers of the same compounds can react with light differently, based simply on the three-dimensional positioning of a meta anisyl ring. The result is that the stereoisomers of the compound with the same configuration at both stereogenic centers are photolabile while the stereoisomers with opposite configuration do not react with light. Furthermore, time-dependent density functional theory (TD-DFT) calculations show distinct excitation pathways for each stereoisomer.

Keywords: diastereoselectivity; photochemistry; protecting groups; diastereodifferentiating

check for updates

Citation: Pham, H.; Hunsley, M.; Yang, C.-H.; Wang, H.; Reed, S.M. Demonstration of a Stereospecific Photochemical Meta Effect. *Photochem* **2022**, *2*, 69–76. https://doi.org/10.3390/photochem2010006

Received: 29 November 2021
Accepted: 27 December 2021
Published: 12 January 2022

Publisher's Note: MDPI stays neutral with regard to jurisdictional claims in published maps and institutional affiliations.

Copyright: © 2022 by the authors. Licensee MDPI, Basel, Switzerland. This article is an open access article distributed under the terms and conditions of the Creative Commons Attribution (CC BY) license (https://creativecommons.org/licenses/by/4.0/).

1. Introduction

The regioselective meta effect was first reported in the photochemical solvolysis of nitrophenyl phosphonate and sulfonate esters [1] and later in a series of *m*- and *p*-isomers of nitrophenyl and cyanophenyl trityl ethers [2]. The meta effect has been used in the design of photoreleasable protecting groups (PPGs) [3,4], including a broad range of chromophores used to protect carbonyl compounds [5,6]. Early calculations showed that excited singlet states of *m*-methoxy-substituted benzylic acetates led to heterolysis and that increasing meta substitution enhanced photolability [7,8]. More recently, we have reported indirect pathways to photocleavage that occur after an ultrafast back electron transfer to the ground electronic state for *m*-methoxy substituted aromatic compounds. For suitably substituted compounds, the electronic-nuclear couplings facilitate sufficient energy transfer to cause a dissociation reaction [9].

While the meta effect has been thought of as a regioselective phenomenon, in principle, a more subtle change in the chromophore, such as a stereochemical change, could also influence whether a bond is photolabile. While differential reactivity to light is well documented in diastereomers, such as is seen in stereoselective bond-forming photoreactions [10–12] and diastereoselective photoisomerization reactions [13], we are aware of no examples in which a change to the absolute configurations of stereocenters results in a bond becoming photolabile.

Here, we report on diastereomers that either do or do not photocleave based on the configuration of their stereogenic centers. This is in contrast to the few known cases of diastereomer differentiating photocleavage reactions where two different products result based on the stereochemistry of the input molecule [10,14,15]. In this diastereomer differentiating reaction, only the stereoisomer with a meta methoxy ring positioned anti to

a third chromophore is photolabile. Given the utility of photolabile bonds in the design of PPGs [16], for patterning surfaces [17], automating DNA synthesis [18], releasing biological substrates [19], and for the design of molecular logic gates and actuators [20,21], the on/off type of reaction reported here is likely to be a useful extension of the meta effect.

2. Synthesis

The synthesis (Scheme 1) utilizes a similar strategy to one reported for derivatizing salicylic acid to form a carbonyl PPG [3] but takes advantage of the fact that nitriles react with only a single equivalent of Grignard reagent, thereby allowing two different groups to be added sequentially to a nitrile and then the resultant ketone, generating an asymmetric center at the benzylic position. Specifically, benzyl protected 2-hydroxy benzonitrile was reacted with the Grignard of *m*-bromoanisole to form ketone **1**. Addition of the Grignard of *p*-bromoanisole to ketone **1** in a subsequent reaction produced alcohol **2**. Removal of the benzyl protecting group to produce diol **3** was accomplished with hydrogen over palladium on carbon. Finally, 3-phenylpropanal and pTSA were added to produce acetal **4** while introducing a second stereogenic center to produce a pair of racemates.

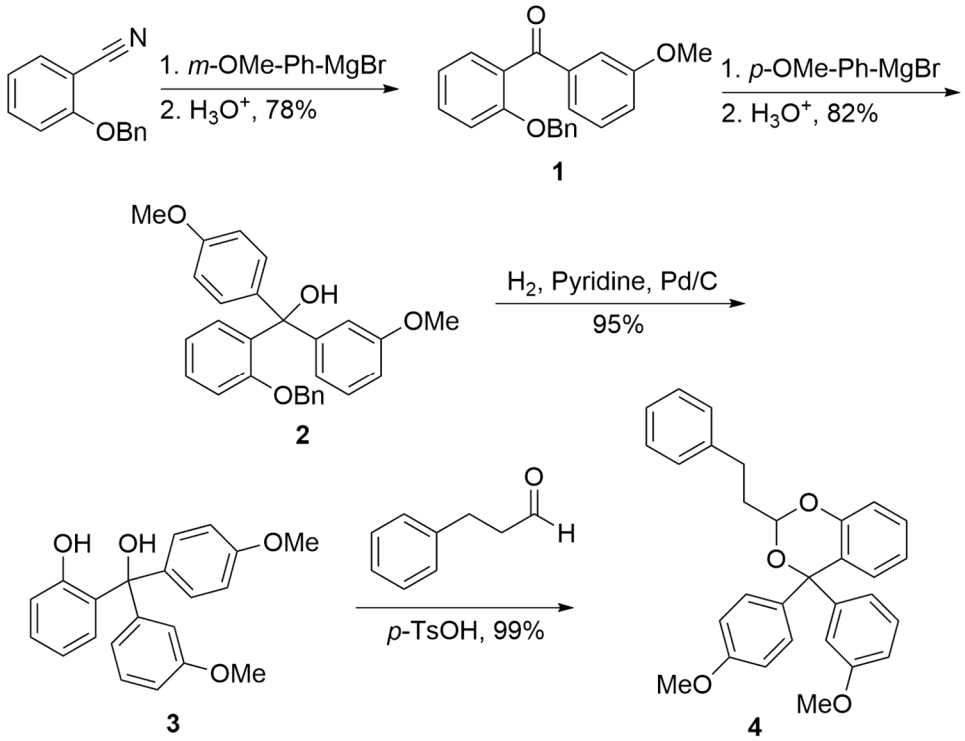

Scheme 1. Synthetic route to acetal stereoisomers.

3. Results

Crystals of **4** were obtained from ethyl acetate and hexanes and the structure determined by x-ray crystallography (see Supplementary Information). The unit cell contained four molecules of (*2S,4R*)-**4** and four molecules of (*2R,4S*)-**4** consistent with the absence of optical activity. The synthesis results in four stereoisomers, two with like stereogenic centers, (*2S,4S*)-**4** and (*2R,4R*)-**4,** and two with unlike stereogenic centers, (*2S,4R*)-**4** and (*2R,4S*)-**4**. The racemate with unlike [22] stereogenic centers (*u*) ((*2S,4R*)-**4** and (*2R,4S*)-**4**) was the predominant form isolated at 76%, with the racemate with like stereogenic centers (*l*) comprising the remaining 24%. The *u* racemate has an acetal ^{13}C NMR peak at 92.45 ppm and was readily distinguishable from the *l* racemate at 92.87 ppm (Figure 1). Similarly, ^{1}H NMR was also used to distinguish the two racemates (see Supplementary Information).

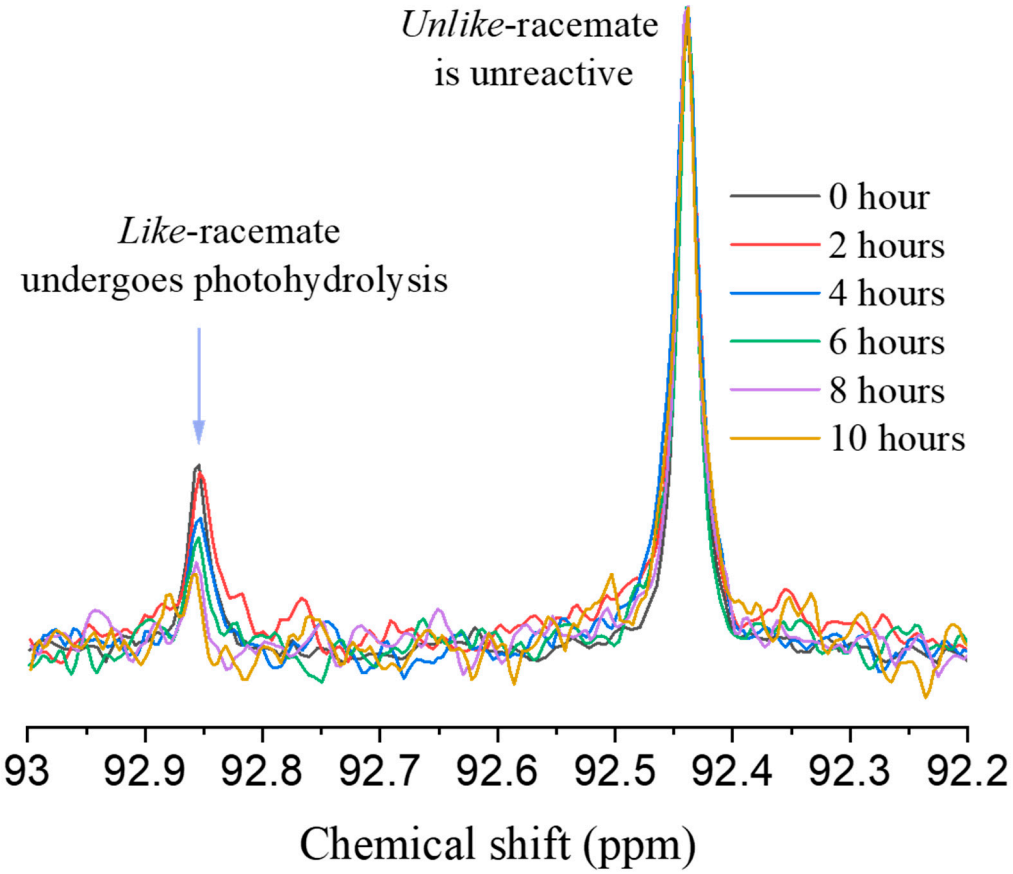

Figure 1. ^{13}C NMR time series taken during irradiation of acetal 4 with UV light.

When a 0.02 M mixture of *l* and *u* racemates was irradiated with UV light from a 75 W Xenon lamp in a 90:10 MeCN:H_2O mixture at room temperature, 3-phenylpropanal and diol 3 were released (Scheme 2). Over 10 h, little photohydrolysis of the *u* racemate at 92.45 ppm was observed whereas 67% of the *l* racemate was converted to 3-phenylpropanal and diol 3 as measured by integrating the ^{13}C acetal peak. A similar trend was observed in the ^{1}H NMR confirming the decrease in the *l* racemate over 10 h although overlap of the two acetal peaks and the two methoxy signals made quantification of the ^{1}H NMR difficult (see Supplementary Information, Figure S2).

Calculations were performed using the quantum chemical program packages Q-Chem [23] and Gaussian 16 [23,24]. For both racemates, the first excited state, S_1, has a stable structure not far away from the ground state Franck–Condon vertical excitation point (the stable structure of S_0). This is illustrated in Table 1, where the reorganization energies are listed for the four stereoisomers with respect to both states S_0 and S_1 (calculation details in Supplementary Information). The reorganizational energies are relatively small compared with the electronic excitation energies. Similarity of the S_0 and S_1 states is also demonstrated by the root-mean-square deviation in the atom locations between S_0 and S_1 being only 0.1507 Å. Generalized Mulliken-Hush (GMH) analysis [25,26] reveals that the electronic couplings are quite large (>50 kcal/mol). From our previous time-dependent density functional theory (TD-DFT) studies of similar systems [9] this suggests an ultrafast (sub-picosecond) internal conversion process upon excitation from S_0 to S_1. Here, the electronic transition associated with the internal conversion process is in the adiabatic regime, which is characterized by (damped) electronic coherence [9]. Thus, photoexcitation acts as an "energy pump": through absorption followed by internal conversion, the photo energy is converted to the nuclear energy that is used to drive the dissociation reaction at the ground state. The efficiency of this "energy pump" depends on the electronic-nuclear coupling, which is illustrated in Figure 2 by the nuclear force vectors at the Franck-Condon

geometries. The more the force vector is aligned with the reaction coordinate for the dissociation reaction, the more likely the cleavage is to occur.

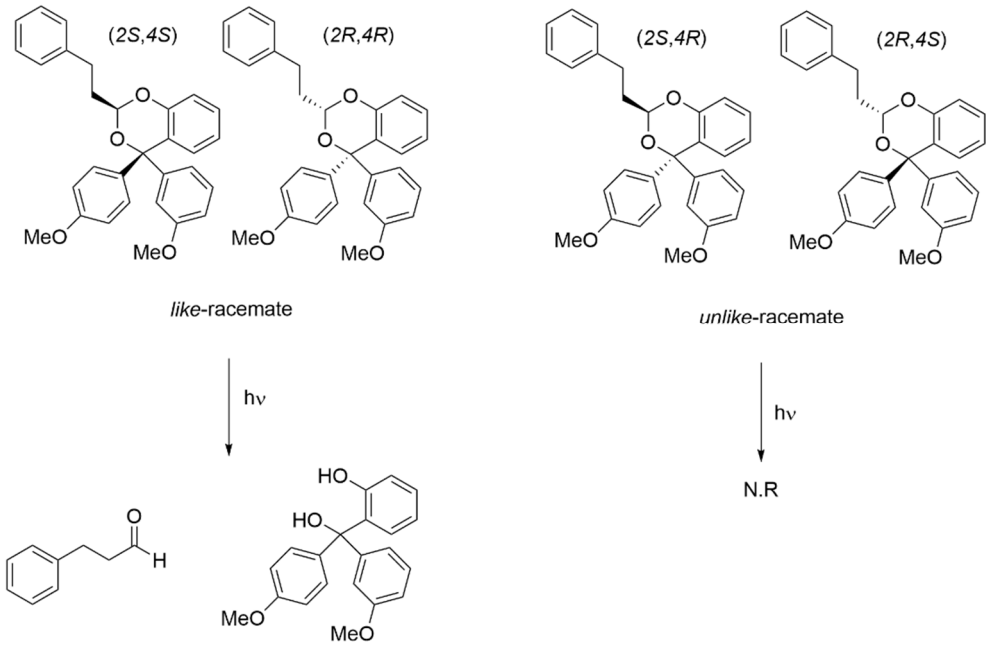

Scheme 2. Stereoselective photorelease.

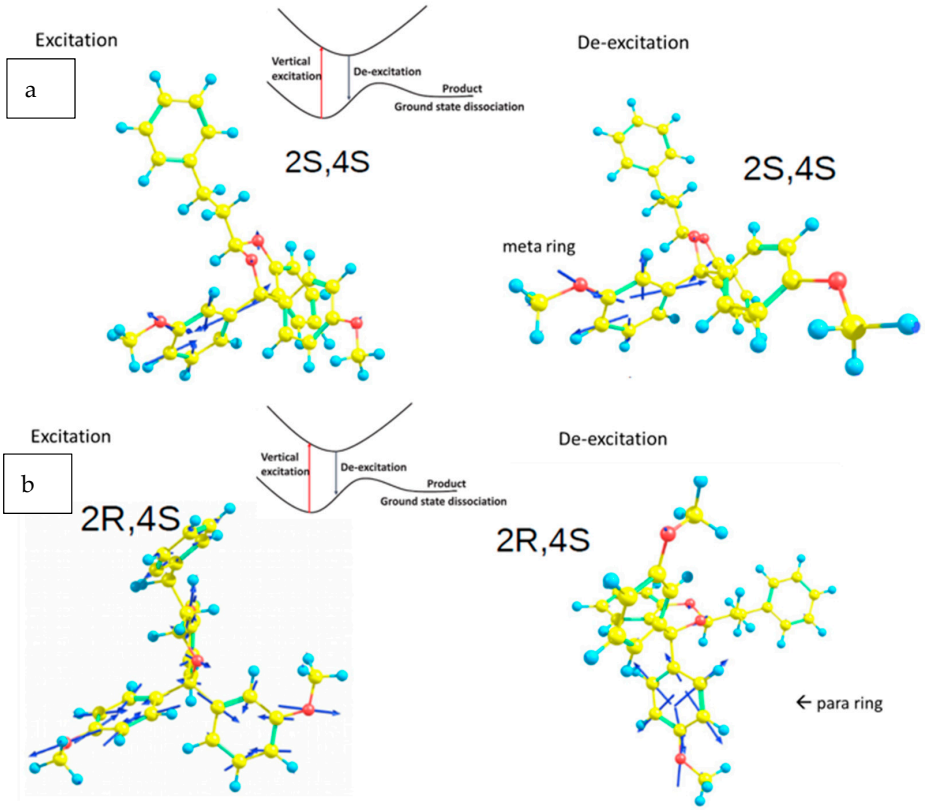

Figure 2. During photohydrolysis, all 4 stereoisomers are present but the lowest energy pathway available varies with the stereochemistry. The reaction pathway is represented from S_0 to S_1 (left) from S_1 to S_0 (right) for the *l* diastereomers (**a**) and the *u* diastereomers (**b**) of **4**. The blue arrows show the vector for the force on each atom during excitation (left) or de-excitation (right) in the lowest energy pathway.

Table 1. Excitation energy (Ex), de-excitation energy (DeEx) and reorganization energies (λ) (kcal/mol) in different electronic states among all stereoisomes. λ ($S_1 \rightarrow S_0$) and λ ($S_0 \rightarrow S_1$) were used for energy difference calculations.

Stereoisomer	Ex (S_1)	λ ($S_1 \rightarrow S_0$)	DeEx (S_1)	λ ($S_0 \rightarrow S_1$)
2R,4R	119.6	3.5	112.8	3.4
2S,4R	120.3	3.1	114.3	2.9
2R,4S	120.3	3.1	114.3	2.9
2S,4S	119.6	3.5	112.8	3.4

When the molecule has two like stereogenic centers, ((*2S,4S*)-4 or (*2R,4R*)-4), the primary excitation pathway involves motion in the meta anisyl ring (Figure 2a). In this case, the meta methoxy ring is positioned anti to the aromatic ring of the phenylethyl group which increases its reactivity. Furthermore, the loss of energy also involves motion that is focused on the meta ring which is known to cause photolability. The overall result is that these structures are more prone to photocleavage. When the molecule has two unlike stereogenic centers, ((*2R,4S*)-4 or (*2S,4R*)-4) and the meta-methoxy ring is syn to the phenylethyl group, the excitation pathway is diffused, involving both the meta and para anisyl rings (Figure 2b). Additionally, here, the loss of energy occurs along with increased motion of atoms in the para substituted rings rather than the meta. In this case, the racemate is not prone to cleavage.

Although stereoselective bond-forming photoreactions [10–12] and distereoselective photoisomerization reactions [13] are somewhat common, analogous bond breaking reactions are not. One example we find of a diastereomer differentiating photocleavage reaction comes from -arylbutyrophenones that alternately undergo Yang cyclization or elimination for different diastereomers [14]. Another example are 3-(2-phthalimido-propionate)-yl PPGs [15] in which the the diastereomer undergoes an E2 elimination to produce a trans alkene in high yield, whereas the erythro compound is unable to populate an antiperiplanar conformation of carboxylate and acetate; therefore, instead, the two groups are removed sequentially in an E1cb mechanism producing a mixture of trans and cis alkene. In both examples there are two different reaction pathways for the different diastereomers. Additionally, the stereogenic centers in those cases are on adjacent carbons whereas here they are on a dioxane ring such that a spacer exists between the stereogenic centers in the 2 and 4 position. In the current system where there is not a second reaction pathway, the molecule either photoreleases its benzylic substituent or it does not. This system, therefore, will be well-suited for applications involving PPGs, surface modifiers, or in vitro or in vivo substrate release. Another category of prior photocleavage examples involve a Norrish type II photoelimination; however, the observed diastereoselectivity originates from a chiral auxiliary [27].

The unique pathway for one diastereomer over the other suggests that interactions between the different aromatic rings are important to the photocleavage mechanism. Either the energy pump is more effective in the *u* racemate with the anti-phenyl ring or de-excitation force in the meta anisyl ring is more aligned with the dissociative reaction coordinate. Conversely for the syn-arranged rings, either the pump is less effective or de-excitation force in the para ring is less aligned with bond dissociation.

4. Discussion and Future Directions

It is likely that other ring systems and other separations between stereogenic centers could result in the same phenomena and that the two stereogenic centers could both be placed on the PPG as opposed to having one originating from the protected substrate as seen here. The inclusion of stereogenic centers on different ring positions could be a general method for creating distance between the stereogenic centers while maintaining communication between the rings. It should be possible to create a set of protecting groups that have identical chemical functionality but with one reactive to both light and

acidity and one reactive to only acidity, creating a simple logic gate with actuator [21]. Other potential applications include monitoring racemizing conditions by the observation of a photoreleased substrate, and racemization could also be used to slowly introduce photolability to a substrate over time.

Alternatively, if both stereogenic centers were contained within the protected substrate, this approach could be used to isolate one diastereomer from the other. Here, achiral light causes diastereomers to react differently due to the arrangement of their chromophores and this suggests that chiral light could in turn affect an enantiospecific transformation using similar compounds which suggests this class of compounds could be used for chiral separations by photoderacemization [28], or that proteins or other chiral environments could be used to induce changes in the stereoselectivity of this reaction [29].

The design of new molecules as stereoselective PPGs can build off the structural lessons learned here as well as the computational techniques. In similar systems, attention to the positioning of aromatic rings near the PPG could again be used to enhance stereoselectivity. For novel compounds, TD-DFT can preview the likely initial steps in the photoreaction pathway. This will facilitate exploration of new chromophores for applications in stereoselective photochemistry.

The fact that two different positionings of the meta ring behaved differently also points out that only a single meta ring is needed to cause this PPG to release. This also demonstrates that communication between the rings, for example by energy transfer, is slow enough that the two positions act independently. This informs new strategies for PPG design and suggests new methods for the design of orthogonal protecting groups [6,30] Additionally, the computational methods described here could be used to predict which stereoisomers would be most likely to react with light.

Supplementary Materials: The following supporting information can be downloaded at: https://www.mdpi.com/article/10.3390/photochem2010006/s1, Figure S1. Crystal structure of (2R,4S)-4-(4-methoxyphenyl)-2-phenethyl-4-(3-methoxyphenyl)-4H-benzo[d][1,3]dioxine; Figure S2. ^{1}H NMR time series taken during 10 h irradiation of a 76:24 (u:l) mixture of acetal 4 with UV; Figure S3. ^{1}H NMR spectrum of (2-(benzyloxy)phenyl)(3-methoxyphenyl)methanone; Figure S4. ^{13}C NMR spectrum of (2-(benzyloxy)phenyl)(3-methoxyphenyl)methanone; Figure S5. ^{1}H NMR spectrum of 2-(benzyloxy)phenyl)(3-methoxyphenyl)(4-methoxyphenyl)methanol; Figure S6. ^{13}C NMR spectrum of 2-(benzyloxy)phenyl)(3-methoxyphenyl)(4-methoxyphenyl)methanol; Figure S7. ^{1}H NMR spectrum of (2-hydroxy(3-methoxyphenyl)(4-methoxy phenyl)methyl)phenol; Figure S8. ^{13}C NMR spectrum of (2-hydroxy(3-methoxyphenyl)(4-methoxy phenyl)methyl)phenol; Figure S9. ^{1}H NMR spectrum of acetal 4, (±)-4-(4-methoxyphenyl)-2-phenethyl-4-(3-methoxyphenyl)-4H-benzo[d][1,3]dioxine; Figure S10. ^{13}C NMR spectrum of 4, (±)-4-(4-methoxyphenyl)-2-phenethyl-4-(3-methoxyphenyl)-4H-benzo[d][1,3]dioxine; Figure S11. IR spectrum of (2-(benzyloxy)phenyl)(3-methoxyphenyl)methanone; Figure S12. IR spectrum of 2-(benzyloxy)phenyl)(3-methoxyphenyl)(4-methoxyphenyl)methanol; Figure S13. IR spectrum of (2-hydroxy(3-methoxyphenyl)(4-methoxy phenyl)methyl)phenol; Figure S14. IR spectrum of (±)-4-(4-methoxyphenyl)-2-phenethyl-4-(3-methoxyphenyl)-4H-benzo[d][1,3]dioxine..

Author Contributions: Conceptualization, S.M.R. and H.W.; synthesis, H.P. and M.H.; methodology and calculations, C.-H.Y.; writing—original draft preparation, H.P.; writing—review and editing, S.M.R., C.-H.Y. and H.W. All authors have read and agreed to the published version of the manuscript.

Funding: NMR instrumentation was supported by NSF grant 1726947. H.P. acknowledges support from the CU Denver EUReCA Program and Undergraduate Research Opportunity Program and SMR acknowledges support from the CU Denver Office of Research Services. H.W. acknowledges the support from the National Science Foundation CHE-1954639. This work used the Extreme Science and Engineering Discovery Environment (XSEDE), which is supported by NSF grant number ACI-1548562, and resources of the National Energy Research Scientific Computing Center (NERSC), which is supported by the Office of Science of the U.S. Department of Energy under Contract No. DE-AC02-05CH11231.

Data Availability Statement: NMR data is provided in the Supplementary Information. X-ray data has been submitted to the Cambridge crystallographic data centre.

Acknowledgments: We thank Brian Newell (CSU) for X-ray crystallographic services.

Conflicts of Interest: The authors declare no conflict of interest.

References

1. Havinga, E.; de Jongh, R.O.; Dorst, W. Photochemical acceleration of the hydrolysis of nitrophenyl phosphates and nitrophenyl sulphates. *Recl. Trav. Chim. Pays-Bas* **1956**, *75*, 378–383. [CrossRef]
2. Zimmerman, H.E.; Somasekhara, S. Mechanistic Organic Photochemistry. III. Excited State Solvolyses. *J. Am. Chem. Soc.* **1963**, *85*, 922–927.
3. Wang, P.; Hu, H.; Wang, Y. Novel photolabile protecting group for carbonyl compounds. *Org. Lett.* **2007**, *9*, 1533–1535. [CrossRef]
4. Yang, H.; Zhang, X.; Zhou, L.; Wang, P. Development of a photolabile carbonyl-protecting group toolbox. *J. Org. Chem.* **2011**, *76*, 2040–2048. [CrossRef]
5. Wang, P.; Hu, H.; Wang, Y. Application of the excited state meta effect in photolabile protecting group design. *Org. Lett.* **2007**, *9*, 2831–2833. [CrossRef]
6. Wang, P.; Wang, Y.; Hu, H.; Spencer, C.; Liang, X.; Pan, L. Sequential removal of photolabile protecting groups for carbonyls with controlled wavelength. *J. Org. Chem.* **2008**, *73*, 6152–6157. [CrossRef]
7. Zimmerman, H.E. The Meta Effect in Organic-Photochemistry-Mechanistic and Exploratory Organic-Photochemistry. *J. Am. Chem. Soc.* **1995**, *117*, 8988–8991.
8. Zimmerman, H.E. The meta-ortho effect in organic photochemistry; Mechanistic and exploratory organic photochemistry. *J. Phys. Chem. A* **1998**, *102*, 5616–5621. [CrossRef]
9. Yang, C.-H.; Denne, J.; Reed, S.; Wang, H. Computational study on the removal of photolabile protecting groups by photochemical reactions. *Comput. Theor. Chem.* **2019**, *1151*, 1–11. [CrossRef]
10. Wrobel, M.N.; Margaretha, P. Diastereomer-differentiating photoisomerization of 5-(cyclopent-2-en-1-yl)-2,5-dihydro-1H-pyrrol-2-ones. *Chem. Commun.* **1998**, *5*, 541–542. [CrossRef]
11. Bach, T.; Hehn, J.P. Photochemical Reactions as Key Steps in Natural Product Synthesis. *Angew. Chem. Int. Ed. Engl.* **2011**, *50*, 1000–1045. [CrossRef]
12. Inoue, Y. Asymmetric photochemical reactions in solution. *Chem. Rev.* **1992**, *92*, 741–770.
13. Cheung, E.; Chong, K.C.; Jayaraman, S.; Ramamurthy, V.; Scheffer, J.R.; Trotter, J. Enantio- and diastereodifferentiating cis,trans-photoisomerization of 2beta,3beta-diphenylcyclopropane-1alpha-carboxylic acid derivatives in organized media. *Org. Lett.* **2000**, *2*, 2801–2804. [CrossRef]
14. Singhal, N.; Koner, A.L.; Mal, P.; Venugopalan, P.; Nau, W.M.; Moorthy, J.N. Diastereomer-differentiating photochemistry of beta-arylbutyrophenones: Yang cyclization versus type II elimination. *J. Am. Chem. Soc.* **2005**, *127*, 14375–14382. [CrossRef]
15. Soldevilla, A.; Griesbeck, A.G. Chiral photocages based on phthalimide photochemistry. *J. Am. Chem. Soc.* **2006**, *128*, 16472–16473. [CrossRef]
16. Klán, P.; Šolomek, T.; Bochet, C.G.; Blanc, A.; Givens, R.; Rubina, M.; Popik, V.; Kostikov, A.; Wirz, J. Photoremovable protecting groups in chemistry and biology: Reaction mechanisms and efficacy. *Chem. Rev.* **2013**, *113*, 119–191. [CrossRef]
17. Romano, A.; Roppolo, I.; Rossegger, E.; Schlögl, S.; Sangermano, M. Recent Trends in Applying Ortho-Nitrobenzyl Esters for the Design of Photo-Responsive Polymer Networks. *Molecules* **2020**, *13*, 2777. [CrossRef]
18. Pirrung, M.C.; Wang, L.; Montague-Smith, M.P. 3′-nitrophenylpropyloxycarbonyl (NPPOC) protecting groups for high-fidelity automated 5′ –> 3′ photochemical DNA synthesis. *Org. Lett.* **2001**, *3*, 1105–1108. [CrossRef]
19. Stensrud, K.; Noh, J.; Kandler, K.; Wirz, J.; Heger, D.; Givens, R.S. Competing pathways in the photo-Favorskii rearrangement and release of esters: Studies on fluorinated p-hydroxyphenacyl-caged GABA and glutamate phototriggers. *J. Org. Chem.* **2009**, *74*, 5219–5227. [CrossRef] [PubMed]
20. Upendar, R.G.; Axthelm, J.; Hoffmann, P.; Taye, N.; Glaser, S.; Gorls, H.; Hopkins, S.L.; Plass, W.; Neugebauer, U.; Bonnet, S.; et al. Co-Registered Molecular Logic Gate with a CO-Releasing Molecule Triggered by Light and Peroxide. *J. Am. Chem. Soc.* **2017**, *139*, 4991–4994.
21. Balzani, V.; Credi, A.; Venturi, M. Molecular logic circuits. *Chemphyschem* **2003**, *4*, 49–59. [CrossRef]
22. Seebach, D.; Prelog, V. The Unambiguous Specification of the Steric Course of Asymmetric Syntheses. *Angew. Chem. Int. Ed. Engl.* **1982**, *9*, 654–660. [CrossRef]
23. Shao, Y.; Gan, Z.; Epifanovsky, E.; Gilbert, A.T.B.; Wormit, M.; Kussmann, J.; Lange, A.W.; Behn, A.; Deng, J.; Feng, X.; et al. Advances in molecular quantum chemistry contained in the Q-Chem 4 program package. *Mol. Phys.* **2015**, *113*, 184–215. [CrossRef]
24. Frisch, M.J.; Trucks, G.W.; Schlegel, H.B.; Scuseria, G.E.; Robb, M.A.; Cheeseman, J.R.; Scalmani, G.; Barone, V.; Petersson, G.A.; Nakatsuji, H.; et al. *Gaussian 16 Rev. C.01*; Gaussian, Inc.: Wallingford, CT, USA, 2016.
25. Cave, R.J.; Newton, M.D. Generalization of the Mulliken-Hush treatment for the calculation of electron transfer matrix elements. *Chem. Phys. Lett.* **1996**, *249*, 15–19. [CrossRef]
26. Cave, R.J.; Newton, M.D. Calculation of electronic coupling matrix elements for ground and excited state electron transfer reactions: Comparison of the generalized Mulliken–Hush and block diagonalization methods. *J. Chem. Phys.* **1997**, *106*, 9213–9226. [CrossRef]

27. Henin, F.; Muzart, J.; Pete, J.-P.; M'boungou-M'passi, A.; Rau, H. Enantioselective Protonation of a Simple Enol: Aminoalcohol-Catalyzed Ketonization of a Photochemically Produced 2-Methylinden-3-ol. *Angew. Chem. Int. Ed. Engl.* **1991**, *30*, 416–418. [CrossRef]
28. Shin, N.Y.; Ryss, J.M.; Zhang, X.; Miller, S.J.; Knowles, R.R. Light-driven deracemization enabled by excited-state electron transfer. *Science* **2019**, *366*, 364–369. [CrossRef] [PubMed]
29. Levi-Minzi, N.; Zandomeneghi, M. Photochemistry in Biological Matrices: Activation of Racemic Mixtures and Interconversion of Enantiomers. *J. Am. Chem. Soc.* **1992**, *114*, 9300–9304. [CrossRef]
30. Bochet, C.G. Orthogonal Photolysis of Protecting Groups. *Angew. Chem. Int. Ed. Engl.* **2001**, *40*, 2071–2073. [CrossRef]